

CamReasoner: Reinforcing Camera Movement Understanding via Structured Spatial Reasoning

Hang Wu¹ Yujun Cai^{2,3,§} Zehao Li⁴ Haonan Ge¹
 Bowen Sun¹ Junsong Yuan⁵ Yiwei Wang¹

¹University of California, Merced

²University of Queensland

³Ant Group

⁴University of Chinese Academy of Sciences

⁵University at Buffalo, State University of New York

[§]Corresponding Author

Abstract

Understanding camera dynamics is a fundamental pillar of video spatial intelligence. However, existing multimodal models predominantly treat this task as a black-box classification, often confusing physically distinct motions by relying on superficial visual patterns rather than geometric cues. We present **CamReasoner**, a framework that reformulates camera movement understanding as a structured inference process to bridge the gap between perception and cinematic logic. Our approach centers on the Observation-Thinking-Answer (O-T-A) paradigm, which compels the model to decode spatio-temporal cues such as trajectories and view frustums within an explicit reasoning block. To instill this capability, we construct a Large-scale Inference Trajectory Suite comprising 18k SFT reasoning chains and 38k RL feedback samples. Notably, we are the **first to employ RL for logical alignment in this domain**, ensuring motion inferences are grounded in physical geometry rather than contextual guesswork. By applying Reinforcement Learning to the Observation-Think-Answer (O-T-A) reasoning paradigm, CamReasoner effectively suppresses hallucinations and achieves state-of-the-art performance across multiple benchmarks.

Date: February 3, 2026

Corresponding: hangwu@ucmerced.edu, vanora.caiyj@gmail.com

Code: <https://github.com/wuhang03/CamReasoner>

Model: <https://huggingface.co/LaurentWu/CamReasoner-7B>

1 Introduction

Camera movement serves as the invisible brushstroke of cinematic storytelling, acting as a vital conduit to convey subtle emotions and orchestrate audience immersion. Whether through Scorsese's seamless tracking shots that create a seductive flow, or Spielberg's dynamic dollies that heighten suspense and awe, these trajectories represent the intentionality of a director shaping the viewer's perception of the physical and emotional world. In the landscape of Multimodal Large Language Models (MLLMs), camera movement understanding has emerged as a critical frontier that bridges the gap between passive pixel perception and active semantic reasoning. From the perspective of understanding, mastering these dynamics allows MLLMs to effectively decouple complex object movements from the observer's ego-motion, even when camera intrinsic parameters are unknown, thereby enabling a more robust comprehension of 3D spatial geometry and narrative intent. This transition from surface-level recognition to deep structural analysis transforms an AI from a mere observer into a cinematic reasoner capable of interpreting the "why" behind every frame. Furthermore, from the perspective of generation, camera movement acts as the essential cornerstone for controllable video synthesis.

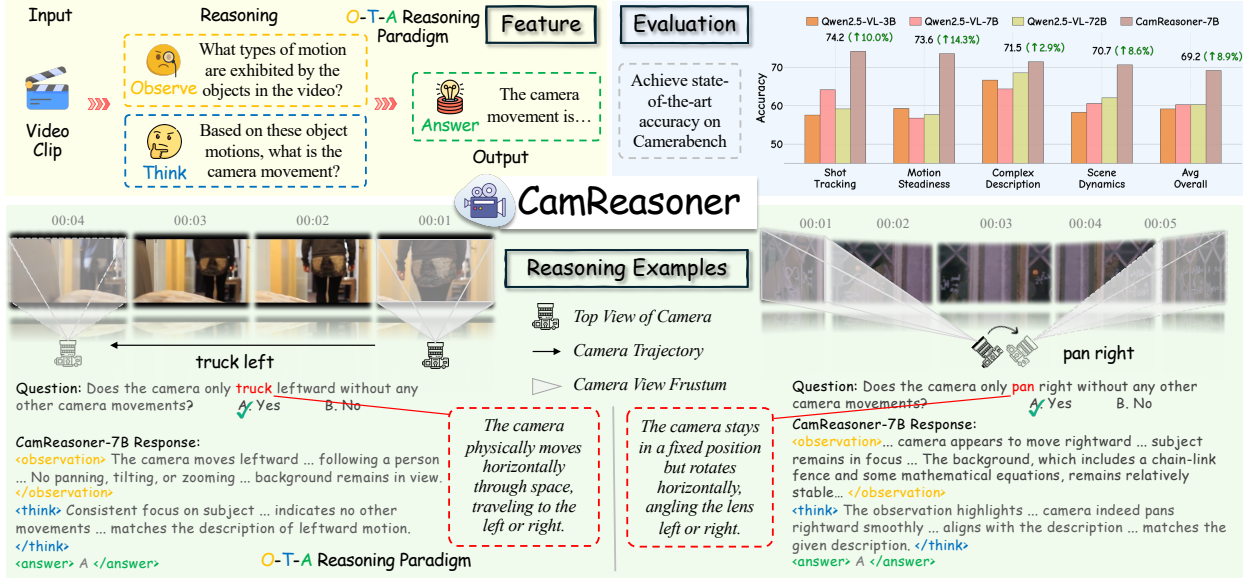


Figure 1 Overview of CamReasoner. We propose the *<observation>-<think>-<answer>* paradigm to improve camera movement understanding. The figure illustrates our model generating detailed visual observations and logical thinking for movements like *truck left* and *pan right*.

As the frontier of AI shifts toward purposeful visual artistry, the ability to generate physically consistent videos relies fundamentally on the model’s grasp of how trajectories interact with scene depth and perspective. By integrating these motion priors, MLLMs can move beyond disorganized pixel synthesis toward achieving true world modeling capabilities, where every shift in perspective is both physically grounded and narratively coherent.

Despite the growing demand for such sophisticated motion perception, current methodologies for camera movement understanding remain split between two constrained paradigms that struggle to meet these requirements. Traditional geometric approaches, such as SfM [34, 39, 52] and SLAM [8, 11], rely on per-frame camera pose estimation to reconstruct trajectories, yet often require prior knowledge of camera intrinsics to maintain accuracy. These systems are fragile in dynamic environments because they often fail to disentangle the camera’s ego-motion from the complex movements of subjects within the scene. In contrast, modern learning-based Video-Language Models (VLMs) [2, 12, 21] offer a promising alternative by treating motion understanding as a semantic task. Leveraging vast pre-training corpora, these models achieve impressive alignment between visual cues and cinematic terminology, while even demonstrating an emerging capacity for high-level reasoning [29]. However, these models predominantly operate as black boxes that leap from pixels to labels without explicit reasoning. This shortcut often triggers hallucinations because the model relies on contextual cues like a running athlete instead of decoding the actual physics of the lens. Consequently, they struggle to distinguish physically distinct yet visually similar operations such as a zoom versus a dolly. These limitations necessitate a framework that bridges the gap between raw perception and structured cinematic logic.

To bridge this gap, we introduce **CamReasoner**, a framework that reformulates camera movement understanding as a structured ego-motion inference task. Central to our approach is the Observation-Thinking-Answer (O-T-A) paradigm, which we implement through a sequential training pipeline of Supervised Fine-Tuning (SFT) and Reinforcement Learning (RL). To support this process, we constructed a Large-scale Inference Trajectory Suite comprising 18k SFT and 38k RL samples. While the SFT data transforms static labels into explainable reasoning chains to instill cinematic logic, the RL samples enforce logical alignment to ground final verdicts in 3D spatio-temporal physics. By explicitly tracing trajectories and analyzing view frustums, our model establishes a rigorous logical premise before delivering a verdict, effectively eliminating contextual guesswork. As the first to apply Reinforcement Learning for logical alignment in this domain, CamReasoner-7B achieves state-of-the-art results, reaching 78.4% in binary classification and 74.5% in VQA. Notably, it excels in challenging Confusable Motion scenarios (60.7%) by distinguishing physical movements like *truck* versus *pan* through geometric reasoning. By integrating structural motion priors, CamReasoner provides a scalable path for MLLMs to achieve precise cinematic control and physically-consistent world modeling.

Our main contributions are summarized as follows:

- **Structured Reasoning Paradigm:** We propose the Observation-Thinking-Answer (O-T-A) paradigm, reformulating camera movement understanding from black-box classification into a structured ego-motion inference task that decouples camera trajectories from dynamic scenes.
- **Inference Trajectory Suite:** We construct a Large-scale Inference Trajectory Suite with 18k SFT and 38k RL samples, transforming static labels into dense reasoning chains to instill spatio-temporal cinematic logic into MLLMs.
- **RL-driven Logical Alignment:** We are the **first to employ Reinforcement Learning** for logical alignment in this domain, achieving state-of-the-art 78.4% and 74.5% accuracy in binary classification and visual question answering tasks.

2 Related Work

2.1 Camera Movement Understanding

Camera movement understanding bridges geometric perception and semantic reasoning, yet current methods face significant bottlenecks. Traditional geometric approaches rely on SfM-based pseudo ground-truth, which is largely restricted to static scenes and ignores scene context [22, 28, 34, 54]. Categorical recognition tasks, while providing semantic labels, often suffer from poor specification—confusing rotation with translation (e.g., pan vs. truck) and failing to capture co-occurring motions in complex cinematography [1, 19, 33]. Although recent benchmarks like ShotBench [29, 45] evaluate nuanced cinematic grammar, existing methodologies lack a structured reasoning process to explain the visual cues driving their interpretations [18, 40]. Consequently, there remains a critical need for a framework that integrates spatial evidence with logical deduction to achieve a holistic understanding across diverse video domains [1, 19, 29, 54].

2.2 Multimodal Reinforcement Learning

Inspired by the reasoning success of LLMs, recent works have extended structured thinking to MLLMs across diverse visual tasks [4, 5, 9, 15, 26, 32, 37, 38, 53]. These include task-specific reasoning models for image VQA [20, 30, 31], video understanding [15, 24], object detection [36, 48], segmentation [47], and temporal grounding [43]. Notably, frameworks like SophiaVL-R1 [14], OneThinker [16], and FrameMind [17] introduce unified reasoning via reinforcement learning, while Thinking-with-Sound [46] extends this paradigm to the audio domain through acoustic tool manipulation. However, despite the surge in RL-based multimodal reasoning, its application to the specialized domain of camera movement understanding remains unexplored.

3 Method

We introduce a two-stage training strategy combining an SFT cold start with Group Relative Policy Optimization (GRPO) [35] to instill the O-T-A reasoning paradigm into camera movement understanding. This pipeline ensures the model efficiently acquires structured reasoning traces while maintaining format adherence and task accuracy. To support this, we curate distinct datasets specifically tailored for sequential Supervised Fine-Tuning and Reinforcement Learning phases.

3.1 Data Collection and Curation

High-quality, structured data is pivotal for teaching the model cinematic logic. We constructed two specialized datasets to facilitate the O-T-A paradigm across the SFT and RL stages.

3.1.1 CamReasoning-SFT-18k Construction.

To instill structured reasoning, we curate the CamReasoning-SFT-18k dataset via an answer-conditioned synthesis pipeline. As shown in Fig. 2, we utilize Qwen2.5-VL-72B to generate 38,672 initial trajectories from original video-QA pairs, enforcing the *<observation>*, *<think>*, and *<answer>* format. To ensure logical coherence, we implement a multi-dimensional filtration process using Qwen3 [2] to verify samples based on format adherence, label accuracy, and

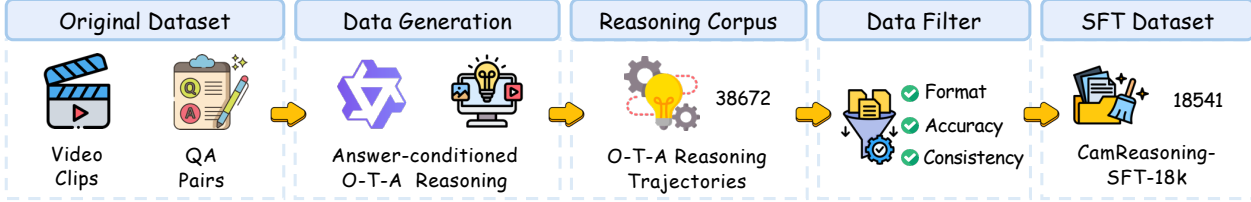


Figure 2 Data generation pipeline for CamReasoning-SFT-18k. We utilize an answer-conditioned process to generate 38,672 initial trajectories, which are then filtered for format, accuracy, and consistency to retain 18,541 high-quality samples.

reasoning consistency. This results in 18,541 high-fidelity samples that serve as cold-start data for teaching the model step-by-step cinematic inference.

3.1.2 CamReasoning-RL-38k

For the reinforcement learning stage, we construct the CamReasoning-RL-38k dataset to drive GRPO [35]. Derived from the CameraBench training split, this dataset provides a diverse array of camera movement scenarios converted into our standardized instruction schema. Unlike the SFT phase, these samples lack reasoning annotations; instead, they serve as environmental queries for the model to refine its self-generated reasoning paths. This setup allows the model to optimize logical robustness and prediction accuracy through trial and error, guided by task-specific reward signals.

3.2 Training Strategy

Our training pipeline comprises two progressive stages designed to endow the model with robust O-T-A reasoning capabilities for camera movement understanding. We first employ SFT as a cold-start initialization to adapt the model to the structured *<observation>-<think>-<answer>* format. Subsequently, we advance to a RL phase utilizing GRPO to further refine the reasoning logic and align outputs with task requirements. Crucially, to mitigate the optimization instability inherent in single-task RL, we incorporate the EMA-GRPO strategy for robust advantage normalization.

3.2.1 Supervised Fine-tuning

We initiate the training process with SFT to bootstrap the model’s capability in generating structured O-T-A (Observation-Think-Answer) reasoning traces. As pre-trained MLLMs lack exposure to our specialized reasoning format encompassing *<observation>*, *<think>*, and *<answer>* tags, SFT provides the essential cold-start initialization. This phase instills adherence to the required formatting and logic patterns, ensuring the model can generate valid reasoning chains and camera movement predictions as defined in our dataset.

Formally, the SFT objective is to minimize the negative log-likelihood of the target sequence o (which explicitly concatenates the observation, reasoning trace, and final answer). Given the input video v and query q , the loss function is formulated as:

$$\mathcal{L}_{\text{SFT}}(\theta) = -\mathbb{E}_{(v, q, o) \sim \mathcal{D}_{\text{SFT}}} \left[\sum_{t=1}^{|o|} \log \pi_{\theta}(o_t | v, q, o_{<t}) \right], \quad (1)$$

where o_t represents the t -th token of the target sequence o , and $o_{<t}$ denotes the preceding tokens. π_{θ} is the policy of the multimodal model parameterized by θ . This stage enables the model to predict each subsequent token conditioned on the visual input, the query, and the generation history, establishing a robust foundation for the subsequent reinforcement learning stage.

3.2.2 Reinforcement Learning Framework

To further align the model’s reasoning capabilities with task requirements and ensure robust logical chains, we employ RL. The training framework is structured into the following components:

Problem Formulation. We formulate the camera movement understanding task as a sequential decision-making process. Given an input video clip v and a textual query q regarding the camera motion, the multimodal policy π_θ generates a structured response sequence o . This output o comprises the visual observation, the explicit reasoning trace, and the final predicted camera movement category. Our optimization objective is to maximize the expected reward of these generated sequences under the policy:

$$J(\theta) = \mathbb{E}_{o \sim \pi_\theta(\cdot|v, q)} [R(o)]. \quad (2)$$

Reward Function Design. Designing an effective reward function is critical for guiding the O-T-A reasoning process. We define a composite reward $R(o)$ that evaluates both the structural validity and the factual correctness of the output. The reward consists of two components: (1) **Format Reward** r_{fmt} : To enforce the strict reasoning structure, we apply a regular expression check. The model receives a reward of 1.0 if and only if the generated output strictly adheres to the sequence of $\langle observation \rangle$, $\langle think \rangle$, and $\langle answer \rangle$ tags; otherwise, $r_{fmt} = 0.0$. (2) **Accuracy Reward** r_{acc} : Conditional on passing the format check, we extract the prediction enclosed within the $\langle answer \rangle$ tags. If the predicted content matches the ground truth camera movement label, r_{acc} is set to a positive score (e.g., 1.0); otherwise, a penalty is applied. If the format check fails, r_{acc} is explicitly set to 0.0.

The final reward $R(o)$ is a weighted interpolation between accuracy and format adherence. Let λ denote the format weight (set to 0.5). The overall reward is formulated as:

$$R(o) = (1 - \lambda) \cdot r_{acc} + \lambda \cdot r_{fmt}. \quad (3)$$

This formulation balances the trade-off between structure adherence and prediction accuracy, ensuring the model learns to generate valid reasoning traces while optimizing for correct answers.

GRPO. To optimize the policy efficiently without the memory overhead of a value network, we utilize the GRPO algorithm. For each query q , we sample a group of G outputs $\{o_1, o_2, \dots, o_G\}$ from the current policy $\pi_{\theta_{old}}$. GRPO estimates the baseline using the group average, avoiding the need for a separate critic model. The training objective is to minimize the following surrogate loss: Let $r_i(\theta) = \frac{\pi_\theta(o_i|q)}{\pi_{\theta_{old}}(o_i|q)}$ be the probability ratio.

$$\mathcal{L}_{GRPO}(\theta) = -\frac{1}{G} \sum_{i=1}^G \left[\min \left(r_i(\theta) A_i, \right. \right. \\ \left. \left. \text{clip}(r_i(\theta), 1 - \epsilon, 1 + \epsilon) A_i \right) - \beta D_{KL} \right], \quad (4)$$

where ϵ is the clipping parameter, A_i is the advantage value, and β controls the strength of the KL divergence penalty D_{KL} (measured against the reference model π_{ref}).

Stability Strategy: EMA-GRPO. To ensure training stability, we adopt the EMA-GRPO [16] strategy for advantage normalization. Standard GRPO normalizes rewards using the immediate batch standard deviation. This introduces significant gradient fluctuations, as low-variance rollouts can lead to artificially inflated advantages and unstable updates. To mitigate this, we employ an exponential moving average (EMA) to estimate a globally stable standard deviation, denoted as $\sigma(t)$. The advantage is computed as:

$$A_i(t) = \frac{R_i - \text{mean}(\{R_j\})}{\sigma(t)}. \quad (5)$$

Here, $\sigma(t)$ captures the intrinsic reward scale and filters out high-frequency noise from individual batches. EMA-GRPO effectively enforces a globally consistent trust region by stabilizing the reward scale, preventing spurious large policy updates caused by accidental low-entropy rollout groups. This approach decouples gradient scaling from immediate rollout randomness and ensures robust convergence during single-task training.

Model	Translation (Dolly/Pedestal/Truck)						Zooming		Rotation (Pan/Tilt/Roll)						Static	Avg
	In	Out	Up	Down	Right	Left	In	Out	Right	Left	Up	Down	CW	CCW		
Random Chance	29.3	9.7	6.7	8.6	15.8	11.5	11.1	10.2	15.0	15.4	12.7	7.7	8.9	10.2	9.7	12.2
<i>SfM/SLAM</i>																
COLMAP [34]	36.2	13.1	11.9	19.7	34.1	30.0	13.9	14.2	43.9	46.4	28.3	19.1	42.1	48.7	7.5	27.3
VGGSLM [39]	56.6	28.9	28.7	38.2	48.9	35.3	21.7	17.3	60.9	58.7	46.6	43.3	61.4	55.5	16.7	41.3
DUSl3R [42]	58.9	24.0	30.7	18.0	38.3	26.9	18.2	24.6	59.4	63.8	32.9	27.3	61.0	57.9	13.1	37.0
MASl3R [10]	47.5	21.1	23.5	40.2	38.7	38.1	42.2	46.6	66.6	58.0	63.2	40.3	50.4	53.5	15.7	43.1
CUTl3R [41]	68.9	50.4	24.7	34.2	37.0	27.6	15.9	21.3	59.1	65.0	65.0	47.5	60.7	66.2	15.1	42.7
MegaSAM [25]	73.8	43.9	24.2	29.1	45.3	44.2	11.1	10.2	79.5	82.2	73.8	65.3	71.5	75.8	22.0	50.1
<i>VQAScore</i>																
LLaVA-OneVision-7B [23]	46.8	13.5	12.6	16.9	23.7	20.2	10.7	14.4	33.5	33.6	16.9	31.4	19.3	20.8	18.8	22.2
LLaVA-Video-7B [51]	54.7	15.2	16.5	19.3	27.1	23.6	16.2	16.9	33.6	36.8	26.9	37.2	16.1	21.7	22.1	25.6
InternVideo2-Chat-8B [44]	69.9	18.5	19.3	17.6	17.9	23.4	12.2	10.4	22.6	22.7	17.2	22.8	19.6	16.4	20.2	22.0
Tarsier-Recap-7B [49]	59.7	15.1	25.7	23.7	28.8	21.5	14.4	15.0	22.8	27.3	24.6	21.6	15.2	18.7	30.7	21.0
InternLMXComposer2.5-7B [50]	49.0	10.6	11.4	10.4	14.6	10.6	11.8	16.5	14.3	13.9	14.7	17.5	11.7	18.1	21.8	16.5
InternVL2.5-8B [6]	67.9	12.9	28.1	25.9	23.4	23.2	18.6	32.1	37.4	30.9	37.6	36.9	11.5	25.3	23.4	29.5
InternVL2.5-26B [6]	63.6	11.8	21.1	23.6	27.2	19.4	21.8	31.6	42.5	38.3	44.9	43.6	14.3	18.2	25.1	29.8
GPT-4o [13]	66.3	29.2	21.1	38.2	38.0	21.9	41.7	39.3	44.7	42.1	43.6	35.5	24.0	28.7	32.0	36.4
InternVL3-8B [55]	61.2	15.5	18.8	29.0	30.5	27.3	29.5	28.1	41.6	49.3	42.0	36.5	21.3	22.3	20.1	31.5
InternVL3-78B [55]	72.0	18.2	19.6	32.5	33.8	29.4	26.4	33.4	47.2	53.5	47.8	40.3	27.6	25.0	22.6	36.8
Qwen2.5-VL-7B [3]	56.0	14.9	18.7	30.5	34.5	27.6	29.8	43.4	62.7	66.7	54.5	34.1	18.8	24.2	19.8	35.8
Qwen2.5-VL-32B [3]	57.6	16.4	20.2	32.1	36.0	29.2	31.4	45.0	64.3	68.2	56.0	35.6	20.2	25.7	21.2	37.3
Qwen2.5-VL-72B [3]	58.0	16.8	20.6	32.5	36.4	29.5	31.7	45.4	64.7	68.6	56.4	36.0	20.6	26.1	21.6	37.7
<i>Previous SOTA</i>																
Cam-Motion-7B [27]	83.9	38.6	27.8	47.8	67.9	50.0	54.5	75.8	79.2	83.8	76.3	67.6	32.3	41.0	73.6	60.0
Cam-Motion-32B [27]	<u>85.6</u>	40.1	29.3	49.4	69.6	51.5	56.0	<u>77.3</u>	80.7	85.4	77.9	69.2	33.9	42.7	75.4	61.6
Cam-Motion-72B [27]	86.8	41.3	30.5	<u>50.6</u>	<u>70.7</u>	52.6	<u>57.1</u>	78.5	<u>81.9</u>	86.6	<u>79.1</u>	<u>70.4</u>	35.0	43.8	<u>76.6</u>	<u>62.8</u>
CamReasoner-7B (Ours)	68.7	57.7	84.9	80.5	84.6	83.2	74.2	72.8	85.7	<u>86.1</u>	87.6	85.7	75.5	<u>70.2</u>	80.1	78.4

Table 1 Binary classification performance on camera movement understanding. **CamReasoner-7B** achieves state-of-the-art results across most categories, significantly outperforming SfM/SLAM baselines and general-purpose MLLMs in average accuracy.

4 Experiments

4.1 Setup

Evaluation Settings We evaluate our model on the CameraBench [27] dataset, focusing on binary classification of motion primitives and the 10K-sample VQA subset covering 9 skills and 81 sub-tasks. To ensure visual grounding, each question is paired with two videos yielding opposite answers. During inference, we standardize video input to a maximum of 64 frames and 262,144 pixels ($128 \times 32 \times 32$) sampled at 1 FPS, with a batch size of 128. This setup evaluates the model across object-centric motion, scene dynamics, and complex logical verification.

Implementation Details The RL phase is implemented using the verl framework with a learning rate of 2×10^{-6} and bf16 mixed-precision. We employ a rollout batch size of 128 and a global batch size of 32. To ensure stability, we incorporate an online filtering mechanism that prunes samples in the top and bottom 1% of the reward distribution. The total reward is defined as $R = r_{acc} + \lambda \cdot r_{fmt}$, with $\lambda = 0.1$. Crucially, the RL policy is initialized from the first SFT epoch to provide a foundational reasoning grasp while maintaining sufficient entropy for exploration.

4.2 Quantitative Results

As presented in Tab. 1, our proposed CamReasoner-7B demonstrates a significant performance leap over a broad spectrum of baseline models, ranging from traditional geometric frameworks to state-of-the-art large vision-language models. Collectively, our model achieves a superior overall accuracy of 78.4%, which not only dramatically outperforms general-purpose benchmarks like GPT-4o (36.4%) and Qwen2.5-VL-72B (37.7%) but also yields a substantial improvement

Model	Motion & Steadiness	Scene Dynamics	Motion Speed	Motion Direction	Confusable Motion	Has Motion	Shot Tracking	Only Motion	Complex Description	Avg Overall
Random Chance	50.0	50.0	50.0	50.0	50.0	50.0	50.0	50.0	50.0	50.0
mPLUG-Owl3-7B	51.8	64.9	61.5	48.6	49.2	54.1	53.2	45.9	63.4	55.8
LLaVA-Video-7B [51]	53.5	66.1	57.2	52.1	49.9	54.9	59.9	51.3	68.0	58.8
LLaVA-OneVision-7B [23]	54.3	63.8	69.0	53.1	55.4	60.9	60.7	43.3	52.3	57.1
InternVideo2-Chat-8B [44]	52.4	64.4	51.7	50.2	49.7	52.2	48.5	50.9	50.6	51.3
Tarsier-Recap-7B [49]	51.8	62.8	50.5	49.8	49.0	51.5	47.8	50.2	49.8	50.6
InternVL2.5-8B [6]	54.4	59.8	57.5	51.3	49.7	58.1	55.2	50.0	50.0	54.5
InternVL2.5-26B [6]	56.2	63.5	60.8	53.8	51.2	60.3	58.4	52.5	53.6	57.2
InternVL3-8B [55]	54.4	59.8	57.5	51.3	49.7	58.1	55.2	50.0	50.0	54.5
InternVL3-78B [55]	56.2	63.5	60.8	53.8	51.2	60.3	58.4	52.5	53.6	57.2
GPT-4o [13]	55.8	52.6	61.2	58.1	53.3	64.1	51.7	42.1	61.9	59.0
Gemini-2-Flash [7]	53.6	46.8	56.6	44.5	41.1	46.5	46.5	39.2	63.8	51.8
Gemini-2.5-Pro [7]	58.2	51.3	60.1	48.9	45.7	52.3	49.7	42.8	64.5	54.7
Qwen2.5-VL-3B [3]	59.3	58.3	60.6	54.0	51.7	55.7	57.6	50.0	66.7	59.2
Qwen2.5-VL-7B [3]	56.8	60.6	62.9	56.9	54.0	58.4	64.2	53.6	64.4	60.3
Qwen2.5-VL-72B [3]	57.7	62.1	71.0	57.8	53.2	62.4	59.2	50.4	68.6	60.3
CamReasoner-7B (Ours)	78.0	77.0	74.1	67.4	60.7	71.8	71.3	60.6	82.6	74.5

Table 2 VQA evaluation on the CameraBench. We compare **CamReasoner-7B** against various state-of-the-art MLLMs across nine fine-grained dimensions. Our model consistently achieves the highest accuracy in all categories, demonstrating superior reasoning capabilities in camera movement understanding.

of 15.6% over the task-specific SFT baseline. This performance gap underscores the model’s exceptional mastery of camera-centric reasoning, particularly in complex rotation and translation tasks. Specifically, CamReasoner-7B establishes new SOTA results in challenging categories such as *Move Up* (84.9%), *Tilt Up* (87.6%), and *Pan Left* (86.1%), suggesting that it has developed a robust spatial-temporal awareness capable of decoupling ego-motion from dynamic scene backgrounds. Furthermore, the model exhibits remarkable resilience in traditionally difficult scenarios like *Move Out* and *Zooming*, where perspective transformations are most aggressive; for instance, it elevates the accuracy of the *Move Out* category to 57.7%, nearly doubling the performance of several competitive baselines. By comparing these results with SFT-only variants, it becomes evident that while supervised learning provides the fundamental paradigm for motion identification, our reinforcement learning phase effectively sharpens the policy’s decision boundaries and maintains high policy entropy during the initial stages to avoid overfitting. Consequently, these results validate that our framework successfully bridges the gap between raw visual perception and high-level camera movement reasoning, providing a robust foundation for automated cinematography analysis.

These findings are further corroborated by the VQA evaluation results presented in Tab. 2. CamReasoner-7B (Ours) maintains its dominance across a diverse array of evaluative dimensions, achieving a superior overall average accuracy of 74.5%. Our model establishes new performance ceilings in critical categories such as Motion & Steadiness (78.0%), Scene Dynamics (77.0%), and Shot Tracking (71.3%). Notably, the model demonstrates exceptional proficiency in identifying complex scenarios, reaching 82.6% in Complex Description and 60.7% in Confusable Motion, significantly outperforming previous state-of-the-art results. Furthermore, it shows high precision in logical reasoning tasks, as evidenced by its performance in Has Motion (71.8%) and Only Motion (60.6%) categories. This consistent outperformance across both binary classification and multidimensional VQA tasks reinforces the model’s robust capacity for high-fidelity camera movement understanding.

4.3 Qualitative Results

The qualitative results in Fig. 3 substantiate the superior performance of CamReasoner-7B in camera movement reasoning. Through a structured *<observation>-<think>-<answer>* pipeline, the model effectively translates fine-grained visual cues into logical deductions.

During the observation phase, the model performs a detailed temporal scan to capture subtle shifts in subject-background

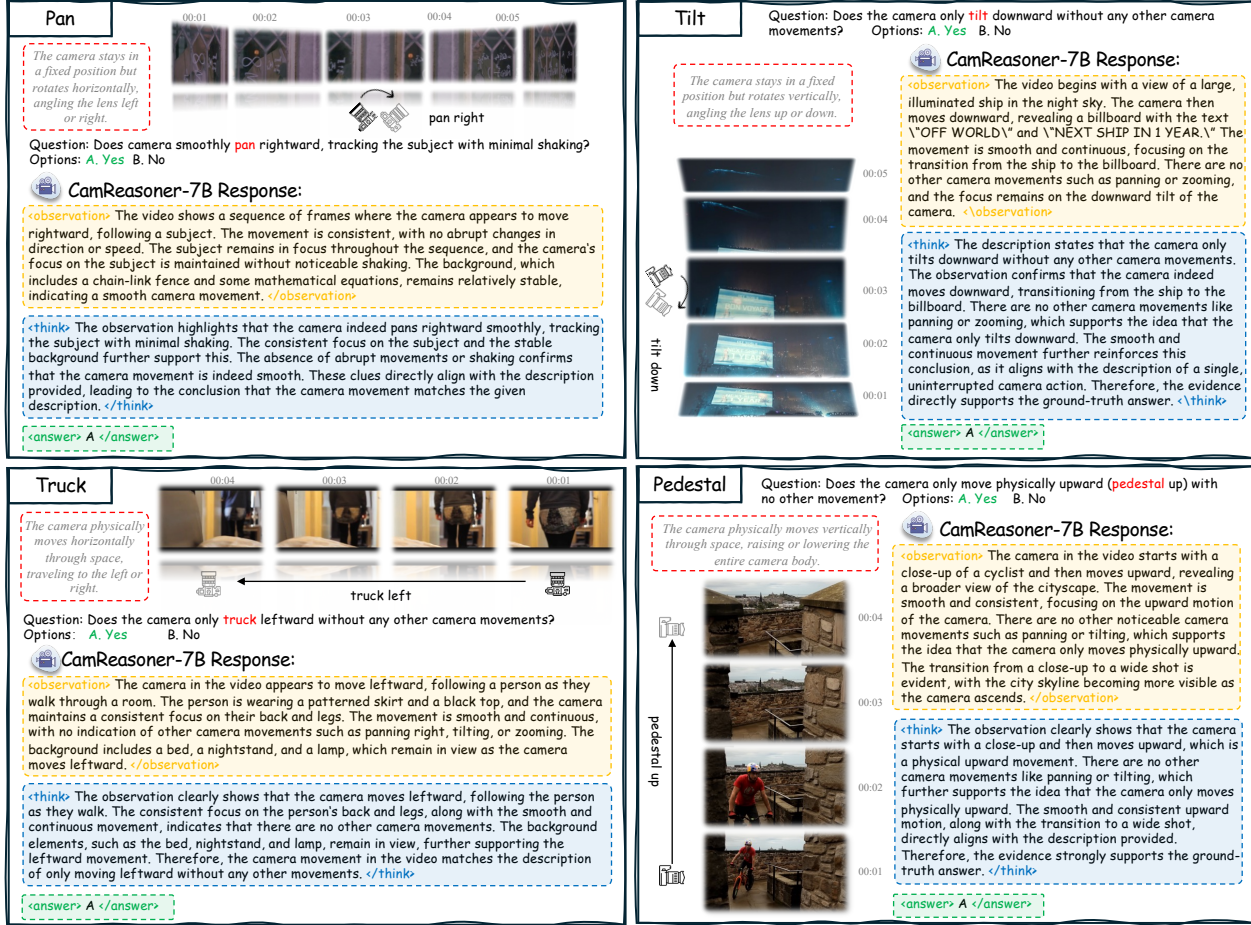


Figure 3 Qualitative results across four typical camera movements. For each case, we visualize the temporal frame sequence alongside the CamReasoner-7B response. The model demonstrates robust spatial reasoning by generating detailed *<observation>* of visual cues and a logical *<think>* process to accurately identify the movement and provide the final *<answer>*.

relations. This granular perception allows it to decouple ego-motion from environmental noise, explicitly describing transitions between visual landmarks. In the subsequent thinking stage, CamReasoner engages in deductive verification grounded in cinematographic principles. By cross-referencing perceived displacements with the absence of confounding rotations, the model demonstrates that it has internalized robust spatial-temporal paradigms rather than relying on superficial statistical correlations.

Finally, the alignment between these textual reasoning chains and the high accuracy underscores the efficacy of our training strategy. By refining a foundational reasoning checkpoint through reinforcement learning, we successfully bridge the gap between low-level visual perception and high-level semantic understanding.

4.4 Training Curves

The training dynamics of the SFTphase exhibit robust convergence and stability, as evidenced by the synchronized progression of loss, gradient norm, and learning rate in Figure 4. Specifically, the training loss undergoes a rapid initial decline and follows a distinct step-wise reduction at each epoch boundary, eventually stabilizing at approximately 0.05, which indicates that the model has effectively captured the underlying distribution of camera movement reasoning tasks. Throughout this process, the gradient norm remains within a well-behaved range between 2.0 and 4.0, ensuring a stable optimization landscape under the peak learning rate of 1.0×10^{-5} and its subsequent cosine decay. Notably, we select the checkpoint from the conclusion of the first epoch as the initialization for the subsequent RL stage; at this juncture, the model has successfully acquired the fundamental paradigms of spatial reasoning and the *<observation>*-*<think>*-

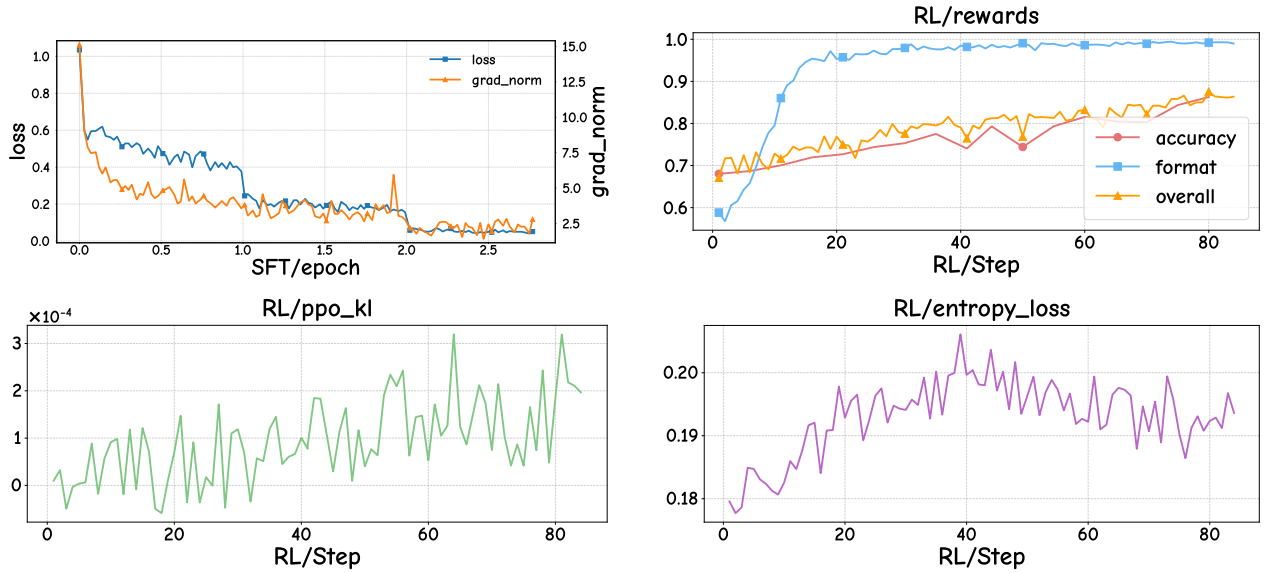


Figure 4 Training curves for SFT and RL phases. The top row shows the loss and grad_norm during the SFT process; the bottom row visualizes the convergence of accuracy, format, and overall rewards during RL training.

<answer>output format, yet retains sufficient policy entropy by avoiding the potential overfitting characteristic of later training stages.

The RL phase, initialized from the first-epoch SFT checkpoint, further refines the model’s policy to achieve rigorous logical alignment. As illustrated in Figure 4, the training dynamics demonstrate a consistent upward trend across all reward metrics. Specifically, the reward/format metric experiences a rapid surge within the first 20 steps, quickly stabilizing near a perfect score of 1.0. This indicates that the model swiftly masters the *<observation>-<think>-<answer>* structural constraint, even under the exploration pressure of the RL environment. Concurrent with format stabilization, the reward/accuracy exhibits a steady and robust climb from approximately 0.68 to over 0.85, proving that the GRPO-based optimization effectively sharpens the model’s camera-centric reasoning boundaries. The synchronized growth of the reward/overall metric, which eventually plateaus at a high equilibrium, confirms the successful balance between linguistic consistency and spatial-temporal accuracy. As shown in the qualitative results, this optimized policy enables CamReasoner-7B to execute meticulous deductive chains—such as explicitly verifying the absence of confounding motions in complex *Truck* or *Pedestal* shots—thereby bridging the gap between raw perception and logical cinematic analysis.

4.5 Ablation Study

Model	SFT	RL	Binary Avg.	VQA Avg.
Base (Qwen2.5-VL-7B)			35.8	60.3
CamReasoner-SFT	✓		68.0	69.5
CamReasoner-7B	✓	✓	78.4	74.5

Table 3 Ablation of training stages. SFT enables structured reasoning, while RL further polishes performance.

We evaluate the impact of training stages and the reward weight λ on CameraBench. As shown in Table 3, the base model shows limited capability in interpreting complex cinematographic motions. Our SFT stage provides a foundational boost by aligning the model with the O-T-A reasoning paradigm, enabling it to decouple camera ego-motion from scene dynamics. The subsequent RL phase yields an additional 10.4% improvement in binary accuracy, demonstrating its effectiveness in optimizing decision-making and enforcing logical consistency across long-range temporal sequences.

Furthermore, Table 4 analyzes the sensitivity of λ , which balances accuracy (r_{acc}) and format (r_{fmt}) rewards. Performance peaks at $\lambda = 0.1$, suggesting that while a small format reward is crucial for stabilizing the reasoning

λ Value	0.0	0.1	0.3	0.5
Binary Acc (%)	76.2	78.4	75.9	71.4
VQA Acc (%)	71.8	74.5	72.1	68.3

Table 4 Ablation study of the reward weight λ . Values represent the Accuracy (%) across different evaluation tasks. A balanced weight of $\lambda = 0.1$ achieves the optimal performance.

structure and ensuring parseable outputs, over-prioritizing formatting at higher values can detract from deep reasoning by constraining the model’s expressive capacity. This indicates that once the structural paradigm is established, the reinforcement signal should primarily focus on the correctness of the spatial-temporal deductions.

5 Conclusions

In this paper, we introduced **CamReasoner**, a framework that reformulates camera movement understanding as a structured ego-motion inference task. By employing the O-T-A paradigm, the model explicitly decouples camera motion from complex backgrounds through spatial-temporal reasoning. Our construction of a Large-scale Inference Trajectory Suite, comprising 18k SFT and 38k RL samples, provides a foundational resource for teaching models cinematic logic. Experimental results show that CamReasoner-7B establishes a new state-of-the-art, achieving 78.4% accuracy in binary classification and outperforming GPT-4o by over 40%. Furthermore, our pioneering use of Reinforcement Learning for logical alignment effectively mitigates hallucinations in challenging scenarios like Confusable Motion. By bridging visual perception and structured deduction, CamReasoner offers a powerful foundation for future advancements in automated film analysis and controllable video synthesis.

References

- [1] Dawit Mureja Argaw, Fabian Caba Heilbron, Joon-Young Lee, Markus Woodson, and In So Kweon. The anatomy of video editing: A dataset and benchmark suite for ai-assisted video editing, 2022. URL <https://arxiv.org/abs/2207.09812>.
- [2] Shuai Bai, Yuxuan Cai, Ruizhe Chen, Keqin Chen, Xionghui Chen, Zesen Cheng, Lianghao Deng, Wei Ding, Chang Gao, Chunjiang Ge, Wenbin Ge, Zhifang Guo, Qidong Huang, Jie Huang, Fei Huang, Binyuan Hui, Shutong Jiang, Zhaohai Li, Mingsheng Li, Mei Li, Kaixin Li, Zicheng Lin, Junyang Lin, Xuejing Liu, Jiawei Liu, Chenglong Liu, Yang Liu, Dayiheng Liu, Shixuan Liu, Dunjie Lu, Ruilin Luo, Chenxu Lv, Rui Men, Lingchen Meng, Xuancheng Ren, Xingzhang Ren, Sibo Song, Yuchong Sun, Jun Tang, Jianhong Tu, Jianqiang Wan, Peng Wang, Pengfei Wang, Qiuyue Wang, Yuxuan Wang, Tianbao Xie, Yiheng Xu, Haiyang Xu, Jin Xu, Zhibo Yang, Mingkun Yang, Jianxin Yang, An Yang, Bowen Yu, Fei Zhang, Hang Zhang, Xi Zhang, Bo Zheng, Humen Zhong, Jingren Zhou, Fan Zhou, Jing Zhou, Yuanzhi Zhu, and Ke Zhu. Qwen3-vl technical report. *arXiv preprint arXiv:2511.21631*, 2025.
- [3] Shuai Bai, Keqin Chen, Xuejing Liu, Jialin Wang, Wenbin Ge, Sibo Song, Kai Dang, Peng Wang, Shijie Wang, Jun Tang, Humen Zhong, Yuanzhi Zhu, Mingkun Yang, Zhaohai Li, Jianqiang Wan, Pengfei Wang, Wei Ding, Zheren Fu, Yiheng Xu, Jiabo Ye, Xi Zhang, Tianbao Xie, Zesen Cheng, Hang Zhang, Zhibo Yang, Haiyang Xu, and Junyang Lin. Qwen2.5-vl technical report, 2025. URL <https://arxiv.org/abs/2502.13923>.
- [4] Shuang Chen, Yue Guo, Zhaochen Su, Yafu Li, Yulun Wu, Jiacheng Chen, Jiayu Chen, Weijie Wang, Xiaoye Qu, and Yu Cheng. Advancing multimodal reasoning: From optimized cold start to staged reinforcement learning. *arXiv preprint arXiv:2506.04207*, 2025.
- [5] Shuang Chen, Yue Guo, Yimeng Ye, Shijue Huang, Wenbo Hu, Haoxi Li, Manyuan Zhang, Jiayu Chen, Song Guo, and Nanyun Peng. Ares: Multimodal adaptive reasoning via difficulty-aware token-level entropy shaping. *arXiv preprint arXiv:2510.08457*, 2025.
- [6] Zhe Chen, Weiyun Wang, Yue Cao, Yangzhou Liu, Zhangwei Gao, Erfei Cui, Jinguo Zhu, Shenglong Ye, Hao Tian, Zhaoyang Liu, Lixin Gu, Xuehui Wang, Qingyun Li, Yiming Ren, Zixuan Chen, Jiapeng Luo, Jiahao Wang, Tan Jiang, Bo Wang, Conghui He, Botian Shi, Xingcheng Zhang, Han Lv, Yi Wang, Wenqi Shao, Pei Chu, Zhongying Tu, Tong He, Zhiyong Wu, Huipeng Deng, Jiaye Ge, Kai Chen, Kaipeng Zhang, Limin Wang, Min Dou, Lewei Lu, Xizhou Zhu, Tong Lu, Dahua Lin, Yu Qiao, Jifeng Dai, and Wenhui Wang. Expanding performance boundaries of open-source multimodal models with model, data, and test-time scaling, 2025. URL <https://arxiv.org/abs/2412.05271>.
- [7] Gheorghe Comanici and Eric Bieber et al. Gemini 2.5: Pushing the frontier with advanced reasoning, multimodality, long context, and next generation agentic capabilities, 2025. URL <https://arxiv.org/abs/2507.06261>.
- [8] Andrew J. Davison, Ian D. Reid, Nicholas D. Molton, and Olivier Stasse. Monoslam: Real-time single camera slam. *IEEE Transactions on Pattern Analysis and Machine Intelligence*, 29(6):1052–1067, 2007. doi: 10.1109/TPAMI.2007.1049.
- [9] Chengqi Duan, Kaiyue Sun, Rongyao Fang, Manyuan Zhang, Yan Feng, Ying Luo, Yufang Liu, Ke Wang, Peng Pei, Xunliang Cai, et al. Codeplot-cot: Mathematical visual reasoning by thinking with code-driven images. *arXiv preprint arXiv:2510.11718*, 2025.
- [10] Bardienus Duisterhof, Lojze Zust, Philippe Weinzaepfel, Vincent Leroy, Yohann Cabon, and Jerome Revaud. Mast3r-sfm: a fully-integrated solution for unconstrained structure-from-motion, 2024. URL <https://arxiv.org/abs/2409.19152>.
- [11] Jakob Engel, Thomas Schöps, and Daniel Cremers. LSD-SLAM: Large-Scale Direct Monocular SLAM. In *European Conference on Computer Vision (ECCV)*, volume 8690 of *Lecture Notes in Computer Science*, pages 834–849, Cham, 2014. Springer International Publishing. ISBN 978-3-319-10604-5. doi: 10.1007/978-3-319-10605-2.
- [12] Comanici et al. Gemini 2.5: Pushing the frontier with advanced reasoning, multimodality, long context, and next generation agentic capabilities. *arXiv preprint arXiv:2507.06261*, 2025.
- [13] OpenAI et al. Gpt-4o system card, 2024. URL <https://arxiv.org/abs/2410.21276>.
- [14] Kaixuan Fan, Kaituo Feng, Haoming Lyu, Dongzhan Zhou, and Xiangyu Yue. Sophiavl-r1: Reinforcing mllms reasoning with thinking reward. *arXiv preprint arXiv:2505.17018*, 2025.
- [15] Kaituo Feng, Kaixiong Gong, Bohao Li, Zonghao Guo, Yibing Wang, Tianshuo Peng, Junfei Wu, Xiaoying Zhang, Benyou Wang, and Xiangyu Yue. Video-r1: Reinforcing video reasoning in mllms. *arXiv preprint arXiv:2503.21776*, 2025.
- [16] Kaituo Feng, Manyuan Zhang, Hongyu Li, Kaixuan Fan, Shuang Chen, Yilei Jiang, Dian Zheng, Peiwen Sun, Yiyuan Zhang, Haoze Sun, et al. Onethinker: All-in-one reasoning model for image and video. *arXiv preprint arXiv:2512.03043*, 2025.

[17] Haonan Ge, Yiwei Wang, Kai-Wei Chang, Hang Wu, and Yujun Cai. Framemind: Frame-interleaved video reasoning via reinforcement learning. *arXiv preprint arXiv:2509.24008*, 2025.

[18] Wenyi Hong, Yean Cheng, Zhuoyi Yang, Weihan Wang, Lefan Wang, Xiaotao Gu, Shiyu Huang, Yuxiao Dong, and Jie Tang. Motionbench: Benchmarking and improving fine-grained video motion understanding for vision language models, 2025. URL <https://arxiv.org/abs/2501.02955>.

[19] Qingqiu Huang, Yu Xiong, Anyi Rao, Jiaze Wang, and Dahu Lin. Movienet: A holistic dataset for movie understanding, 2020. URL <https://arxiv.org/abs/2007.10937>.

[20] Wenzuan Huang, Bohan Jia, Zijie Zhai, Shaosheng Cao, Zheyu Ye, Fei Zhao, Zhe Xu, Yao Hu, and Shaohui Lin. Vision-r1: Incentivizing reasoning capability in multimodal large language models. *arXiv preprint arXiv:2503.06749*, 2025.

[21] Aaron Hurst, Adam Lerer, Adam P Goucher, Adam Perelman, Aditya Ramesh, Aidan Clark, AJ Ostrow, Akila Welihinda, Alan Hayes, Alec Radford, et al. Gpt-4o system card. *arXiv preprint arXiv:2410.21276*, 2024.

[22] Linyi Jin, Richard Tucker, Zhengqi Li, David Fouhey, Noah Snavely, and Aleksander Holynski. Stereo4d: Learning how things move in 3d from internet stereo videos, 2025. URL <https://arxiv.org/abs/2412.09621>.

[23] Bo Li, Yuanhan Zhang, Dong Guo, Renrui Zhang, Feng Li, Hao Zhang, Kaichen Zhang, Peiyuan Zhang, Yanwei Li, Ziwei Liu, and Chunyuan Li. Llava-onevision: Easy visual task transfer, 2024. URL <https://arxiv.org/abs/2408.03326>.

[24] Xinhao Li, Ziang Yan, Desen Meng, Lu Dong, Xiangyu Zeng, Yinan He, Yali Wang, Yu Qiao, Yi Wang, and Limin Wang. Videochat-r1: Enhancing spatio-temporal perception via reinforcement fine-tuning. *arXiv preprint arXiv:2504.06958*, 2025.

[25] Zhengqi Li, Richard Tucker, Forrester Cole, Qianqian Wang, Linyi Jin, Vickie Ye, Angjoo Kanazawa, Aleksander Holynski, and Noah Snavely. Megasam: Accurate, fast, and robust structure and motion from casual dynamic videos, 2024. URL <https://arxiv.org/abs/2412.04463>.

[26] Zongzhao Li, Zongyang Ma, Mingze Li, Songyou Li, Yu Rong, Tingyang Xu, Ziqi Zhang, Deli Zhao, and Wenbing Huang. Star-r1: Spatial transformation reasoning by reinforcing multimodal llms. *arXiv preprint arXiv:2505.15804*, 2025.

[27] Zhiqiu Lin, Siyuan Cen, Daniel Jiang, Jay Karhade, Hewei Wang, Chancharik Mitra, Tiffany Ling, Yuhan Huang, Sifan Liu, Mingyu Chen, et al. Towards understanding camera motions in any video. *arXiv preprint arXiv:2504.15376*, 2025.

[28] Lu Ling, Yichen Sheng, Zhi Tu, Wentian Zhao, Cheng Xin, Kun Wan, Lantao Yu, Qianyu Guo, Zixun Yu, Yawen Lu, Xuanmao Li, Xingpeng Sun, Rohan Ashok, Aniruddha Mukherjee, Hao Kang, Xiangrui Kong, Gang Hua, Tianyi Zhang, Bedrich Benes, and Aniket Bera. Dl3dv-10k: A large-scale scene dataset for deep learning-based 3d vision. In *Proceedings of the IEEE/CVF Conference on Computer Vision and Pattern Recognition (CVPR)*, pages 22160–22169, June 2024.

[29] Hongbo Liu, Jingwen He, Yi Jin, Dian Zheng, Yuhao Dong, Fan Zhang, Ziqi Huang, Yinan He, Yangguang Li, Weichao Chen, Yu Qiao, Wanli Ouyang, Shengjie Zhao, and Ziwei Liu. Shotbench: Expert-level cinematic understanding in vision-language models, 2025. URL <https://arxiv.org/abs/2506.21356>.

[30] Lingrui Mei, Shenghua Liu, Yiwei Wang, Baolong Bi, Yuyao Ge, Jun Wan, Yurong Wu, and Xueqi Cheng. a1: Steep test-time scaling law via environment augmented generation. *arXiv preprint arXiv:2504.14597*, 2025.

[31] Lingrui Mei, Jiayu Yao, Yuyao Ge, Yiwei Wang, Baolong Bi, Yujun Cai, Jiazh Li, Mingyu Li, Zhong-Zhi Li, Duzhen Zhang, Chenlin Zhou, Jiayi Mao, Tianze Xia, Jiafeng Guo, and Shenghua Liu. A survey of context engineering for large language models, 2025. URL <https://arxiv.org/abs/2507.13334>.

[32] Jiahao Meng, Xiangtai Li, Haochen Wang, Yue Tan, Tao Zhang, Lingdong Kong, Yunhai Tong, Anran Wang, Zhiyang Teng, Yujing Wang, et al. Open-o3 video: Grounded video reasoning with explicit spatio-temporal evidence. *arXiv preprint arXiv:2510.20579*, 2025.

[33] Anyi Rao, Jiaze Wang, Lining Xu, Xuekun Jiang, Qingqiu Huang, Bolei Zhou, and Dahu Lin. A unified framework for shot type classification based on subject centric lens, 2020. URL <https://arxiv.org/abs/2008.03548>.

[34] Johannes L. Schonberger and Jan-Michael Frahm. Structure-from-motion revisited. In *Proceedings of the IEEE Conference on Computer Vision and Pattern Recognition (CVPR)*, June 2016.

[35] Zhihong Shao, Peiyi Wang, Qihao Zhu, Runxin Xu, Junxiao Song, Xiao Bi, Haowei Zhang, Mingchuan Zhang, Y. K. Li, Y. Wu, and Daya Guo. Deepseekmath: Pushing the limits of mathematical reasoning in open language models, 2024. URL <https://arxiv.org/abs/2402.03300>.

[36] Haozhan Shen, Peng Liu, Jingcheng Li, Chunxin Fang, Yibo Ma, Jiajia Liao, Qiaoli Shen, Zilun Zhang, Kangjia Zhao, Qianqian Zhang, et al. Vlm-r1: A stable and generalizable r1-style large vision-language model. *arXiv preprint arXiv:2504.07615*, 2025.

[37] Haoyuan Sun, Jiaqi Wu, Bo Xia, Yifu Luo, Yifei Zhao, Kai Qin, Xufei Lv, Tiantian Zhang, Yongzhe Chang, and Xueqian Wang. Reinforcement fine-tuning powers reasoning capability of multimodal large language models. *arXiv preprint arXiv:2505.18536*, 2025.

[38] Peiwen Sun, Shiqiang Lang, Dongming Wu, Yi Ding, Kaituo Feng, Huadai Liu, Zhen Ye, Rui Liu, Yun-Hui Liu, Jianan Wang, et al. Spacevista: All-scale visual spatial reasoning from mm to km. *arXiv preprint arXiv:2510.09606*, 2025.

[39] Jianyuan Wang, Nikita Karaev, Christian Rupprecht, and David Novotny. Vggsfm: Visual geometry grounded deep structure from motion. In *Proceedings of the IEEE/CVF conference on computer vision and pattern recognition*, pages 21686–21697, 2024.

[40] Jiawei Wang, Liping Yuan, Yuchen Zhang, and Haomiao Sun. Tarsier: Recipes for training and evaluating large video description models, 2024. URL <https://arxiv.org/abs/2407.00634>.

[41] Qianqian Wang, Yifei Zhang, Aleksander Holynski, Alexei A. Efros, and Angjoo Kanazawa. Continuous 3d perception model with persistent state, 2025. URL <https://arxiv.org/abs/2501.12387>.

[42] Shuzhe Wang, Vincent Leroy, Yohann Cabon, Boris Chidlovskii, and Jerome Revaud. Dust3r: Geometric 3d vision made easy, 2024. URL <https://arxiv.org/abs/2312.14132>.

[43] Ye Wang, Ziheng Wang, Boshen Xu, Yang Du, Kejun Lin, Zihan Xiao, Zihao Yue, Jianzhong Ju, Liang Zhang, Dingyi Yang, et al. Time-r1: Post-training large vision language model for temporal video grounding. *arXiv preprint arXiv:2503.13377*, 2025.

[44] Yi Wang, Kunchang Li, Xinhao Li, Jiashuo Yu, Yinan He, Chenting Wang, Guo Chen, Baoqi Pei, Ziang Yan, Rongkun Zheng, Jilan Xu, Zun Wang, Yansong Shi, Tianxiang Jiang, Songze Li, Hongjie Zhang, Yifei Huang, Yu Qiao, Yali Wang, and Limin Wang. Internvideo2: Scaling foundation models for multimodal video understanding, 2024. URL <https://arxiv.org/abs/2403.15377>.

[45] Hang Wu, Yujun Cai, Haonan Ge, Hongkai Chen, Ming-Hsuan Yang, and Yiwei Wang. Refineshot: Rethinking cinematography understanding with foundational skill evaluation. *arXiv preprint arXiv:2510.02423*, 2025.

[46] Zhen Xiong, Yujun Cai, Zhecheng Li, Junsong Yuan, and Yiwei Wang. Thinking with sound: Audio chain-of-thought enables multimodal reasoning in large audio-language models. *arXiv preprint arXiv:2509.21749*, 2025.

[47] Zuyao You and Zuxuan Wu. Seg-r1: Segmentation can be surprisingly simple with reinforcement learning. *arXiv preprint arXiv:2506.22624*, 2025.

[48] En Yu, Kangheng Lin, Liang Zhao, Jisheng Yin, Yana Wei, Yuang Peng, Haoran Wei, Jianjian Sun, Chunrui Han, Zheng Ge, et al. Perception-r1: Pioneering perception policy with reinforcement learning. *arXiv preprint arXiv:2504.07954*, 2025.

[49] Liping Yuan, Jiawei Wang, Haomiao Sun, Yuchen Zhang, and Yuan Lin. Tarsier2: Advancing large vision-language models from detailed video description to comprehensive video understanding, 2025. URL <https://arxiv.org/abs/2501.07888>.

[50] Pan Zhang, Xiaoyi Dong, Yuhang Zang, Yuhang Cao, Rui Qian, Lin Chen, Qipeng Guo, Haodong Duan, Bin Wang, Linke Ouyang, Songyang Zhang, Wenwei Zhang, Yining Li, Yang Gao, Peng Sun, Xinyue Zhang, Wei Li, Jingwen Li, Wenhui Wang, Hang Yan, Conghui He, Xingcheng Zhang, Kai Chen, Jifeng Dai, Yu Qiao, Dahua Lin, and Jiaqi Wang. Internlm-xcomposer-2.5: A versatile large vision language model supporting long-contextual input and output, 2024. URL <https://arxiv.org/abs/2407.03320>.

[51] Yuanhan Zhang, Jinming Wu, Wei Li, Bo Li, Zejun Ma, Ziwei Liu, and Chunyuan Li. Llava-video: Video instruction tuning with synthetic data, 2025. URL <https://arxiv.org/abs/2410.02713>.

[52] Zuobai Zhang, Minghao Xu, Arian Jamasb, Vijil Chenthamarakshan, Aurelie Lozano, Payel Das, and Jian Tang. Protein representation learning by geometric structure pretraining, 2023. URL <https://arxiv.org/abs/2203.06125>.

[53] Guanghao Zhou, Panjia Qiu, Cen Chen, Jie Wang, Zheming Yang, Jian Xu, and Minghui Qiu. Reinforced mllm: A survey on rl-based reasoning in multimodal large language models. *arXiv preprint arXiv:2504.21277*, 2025.

[54] Tinghui Zhou, Richard Tucker, John Flynn, Graham Fyffe, and Noah Snavely. Stereo magnification: Learning view synthesis using multiplane images, 2018. URL <https://arxiv.org/abs/1805.09817>.

[55] Jinguo Zhu, Weiyun Wang, Zhe Chen, Zhaoyang Liu, Shenglong Ye, Lixin Gu, Hao Tian, Yuchen Duan, Weijie Su, Jie Shao, Zhangwei Gao, Erfei Cui, Xuehui Wang, Yue Cao, Yangzhou Liu, Xinguang Wei, Hongjie Zhang, Haomin Wang, Weiye Xu, Hao Li, Jiahao Wang, Nianchen Deng, Songze Li, Yinan He, Tan Jiang, Jiapeng Luo, Yi Wang, Conghui He, Botian Shi, Xingcheng Zhang, Wenqi Shao, Junjun He, Yingtong Xiong, Wenwen Qu, Peng Sun, Penglong Jiao, Han Lv, Lijun Wu, Kaipeng Zhang, Huipeng Deng, Jiaye Ge, Kai Chen, Limin Wang, Min Dou, Lewei Lu, Xizhou Zhu, Tong Lu, Dahua Lin, Yu Qiao,

Jifeng Dai, and Wenhui Wang. Internvl3: Exploring advanced training and test-time recipes for open-source multimodal models, 2025. URL <https://arxiv.org/abs/2504.10479>.

